R-matrix theory of photoionization. Application to neon and argon

J. Phys. B: Atom. Molec. Phys., Vol. 8, No. 16, 1975. Printed in Great Britain.

R-matrix theory of photoionization. Application to neon and argon

P G Burke and K T Taylor

Department of Applied Mathematics and Theoretical Physics, The Queen's University of Belfast, Belfast BT7 1NN, N Ireland

Received 6 June 1975

Abstract. The *R*-matrix method, which has been used recently to calculate electron–atom and ion collision cross sections and atomic polarizabilities is extended to enable atomic photoionization processes to be studied. Both the initial atomic bound state and the final atomic continuum state are expanded in terms of *R*-matrix bases. The method is programmed for a general atomic system and then used to calculate the photoionization cross sections of ground state neon and argon atoms leaving the residual ions in their ground or first excited states. Good agreement is obtained with recent experiments using synchrotron radiation both in resonant and non-resonant regions, showing that the method has a wide range of applicability.

1. Introduction

In the last few years there has been a very considerable increase in experimental and theoretical interest in the photoionization of atomic gases. On the experimental side this has been stimulated by the ready availability of synchrotron radiation sources enabling accurate measurements to be carried out over the whole spectral range from the visible to the x-ray region. On the theoretical side many-body methods are being increasingly applied enabling accurate predictions for atomic systems to be made and giving a new understanding of the dynamics of photoionization processes (Fano and Cooper 1968).

In this paper we describe the first detailed application of the *R*-matrix method to atomic photoionization processes. The *R*-matrix method has so far been mainly applied to electron–atom and electron–ion collisions where cross sections for a considerable number of target atoms and ions including H, He, C, N, O, Mg, N^+ and O^+ have been obtained. However, as emphasized by Burke and Robb (1975), the *R*-matrix method can be used as the basis of a very general approach for a broad range of atomic continuum processes including atomic polarizabilities, photoionization cross sections, van der Waals coefficients and non-linear optical coefficients. In addition, because of the generality of the approach, it is possible to design and implement a series of general computer program packages which will enable all of these processes to be calculated for a general atomic system (Berrington *et al* 1974).

Our plan in the following sections is therefore to first develop the general *R*-matrix theory of photoionization and then to test the theory, and the computer programs which have been written to implement the theory, by calculating cross sections for the photoionization of neon and argon. Our choice of these atomic systems is motivated both by

the wealth of accurate data now available, and also by the fact that a considerable number of other theoretical studies have been carried out with which comparison can be made. However, at the same time, we believe that our approach gives an overall description of photoionization in resonant and non-resonant regions which is more consistent than many earlier treatments and is therefore of interest in its own right.

2. *R*-matrix theory of photoionization

The way in which the *R*-matrix theory of atomic polarizabilities can be extended to describe atomic photoionization processes was indicated briefly by Allison *et al* (1972). In this section we develop this theory and show how it relates to the earlier work of Burke *et al* (1971) (to be referred to as BHR) on electron scattering by complex atoms.

The differential cross section for photoionization of an $(N+1)$-electron atom or ion, with the ejection of the electron in the $\hat{\boldsymbol{k}}$ direction, is given in the dipole length approximation by

$$\frac{\mathrm{d}\sigma_{\mathrm{L}}}{\mathrm{d}\hat{\boldsymbol{k}}} = 8\pi^2\alpha a_0^2\omega\left|\left\langle \Psi_f^-(\hat{\boldsymbol{k}}) \left| \sum_{j=1}^{N+1} z_j \right| \Psi_i \right\rangle\right|^2 \tag{1}$$

and in the dipole velocity approximation by

$$\frac{\mathrm{d}\sigma_{\mathrm{V}}}{\mathrm{d}\hat{\boldsymbol{k}}} = \frac{8\pi^2\alpha a_0^2}{\omega}\left|\left\langle \Psi_f^-(\hat{\boldsymbol{k}}) \left| \sum_{j=1}^{N+1} \frac{\partial}{\partial z_j} \right| \Psi_i \right\rangle\right|^2. \tag{2}$$

In these equations, ω is the incident photon energy in atomic units, α is the fine-structure constant, a_0 is the Bohr radius of the hydrogen atom and Ψ_i and $\Psi_f^-(\hat{\boldsymbol{k}})$ are the initial and final continuum wavefunctions. The boundary condition satisfied by $\Psi_f^-(\hat{\boldsymbol{k}})$, which has been discussed in detail by Henry and Lipsky (1967), corresponds to a plane wave in direction $\hat{\boldsymbol{k}}$ incident on the final state of the ion, with ingoing waves in all open channels. In *L–S* coupling, which we use in this paper, $\Psi_f^-(\hat{\boldsymbol{k}})$ can be expanded in the form

$$\Psi_f^-(\hat{\boldsymbol{k}}) = \sum_{l_f m_{l_f} L} \mathrm{i}^{l_f} \exp(-\mathrm{i}\sigma_{l_f}) Y_{l_f}^{m_{l_f}*}(\hat{\boldsymbol{k}}) C_{L_f l_f}(LM_L; M_{L_f} m_{l_f}) C_{S_f \frac{1}{2}}(SM_S; M_{S_f} \tfrac{1}{2}) \Psi_f^- \tag{3}$$

where Ψ_f^- is an eigenstate of total orbital angular momentum L and total spin angular momentum S, which is determined as described below, the $C_{j_1 j_2}(j_{12} m_{12}; m_1 m_2)$ are Clebsch–Gordan coefficients, $L_f S_f M_{L_f} M_{S_f}$ are the quantum numbers defining the final state of the ion, $Y_{l_f}^{m_{l_f}}(\hat{\boldsymbol{k}})$ is the spherical harmonic defined by Rose (1957) describing the ejected electron and $\sigma_{l_f} = \arg\Gamma(l_f + 1 + \mathrm{i}\eta_f)$ with $\eta_f = -(Z-N)/k_f$ where Z is the nuclear charge.

In our application of the *R*-matrix method both Ψ_i in equations (1) and (2) and Ψ_f^- in equation (3) are expanded within some spherical region surrounding the atom in terms of *R*-matrix basis functions defined by

$$\Psi_k(x_1 \ldots x_N) = \mathscr{A} \sum_{ij} c_{ijk} \bar{\Phi}_i(x_1 x_2 \ldots x_N \hat{\boldsymbol{r}}_{N+1} \sigma_{N+1}) u_{ij}(r_{N+1}) + \sum_j d_{jk} \phi_j(x_1 \ldots x_{N+1}). \tag{4}$$

In this equation $\mathscr{A}$ is the antisymmetrization operator, the $\bar{\Phi}_i$ are channel functions consisting of configuration-interaction wavefunctions for the residual ion coupled with spin-angle functions for the $(N+1)$th electron to give an eigenstate of L and S, and the ϕ_j are $(N+1)$-electron bound configurations which are eigenstates with the same L and S which are included to allow for electron correlation effects. Finally, the u_{ij} are

solutions of the zero-order radial differential equation

$$\left(\frac{\mathrm{d}^2}{\mathrm{d}r^2}-\frac{l_i(l_i+1)}{r^2}+V(r)+k_i^2\right)u_{ij}(r)=\sum_k \lambda_{ijk}P_k(r) \tag{5}$$

satisfying the boundary conditions

$$u_{ij}(0)=0$$
$$\frac{a}{u_{ij}}\frac{\mathrm{d}u_{ij}}{\mathrm{d}r}\bigg|_{r=a}=b. \tag{6}$$

The Lagrange undetermined multipliers λ_{ijk} ensure that the continuum orbitals are orthogonal to bound orbitals with the same angular symmetry, $V(r)$ is some appropriately chosen zero-order potential, b is a constant which in our work is taken to be zero and a is the radius of the sphere defining the internal region chosen so that the functions $\overline{\Phi}_i$ and ϕ_j are effectively zero when $r > a$. A detailed discussion of the solution of this equation has been given by Robb (1970).

The coefficients c_{ijk} and d_{jk} in equation (4) are determined by diagonalizing the $(N+1)$-electron Hamiltonian in the internal region. If we write equation (4) in the more convenient form

$$\Psi_k=\sum_{k'}\Phi_{k'}V_{k'k}, \tag{7}$$

where the Φ_k denote collectively the basis functions $\mathscr{A}\overline{\Phi}_i u_{ij}$ and ϕ_j and the $V_{k'k}$ denote collectively the coefficients c_{ijk} and d_{jk}; then these coefficients are given by the eigenvalue equation

$$\sum_{kk'}V_{kk''}(\Phi_k|H|\Phi_{k'})V_{k'k'''}=E_{k''}\delta_{k''k'''} \tag{8}$$

where the round brackets indicate that the radial integrals are taken only over the internal region.

We now expand Ψ_i and Ψ_f^- as follows

$$\Psi_i=\sum_k \Psi_k A_{ki} \tag{9}$$

and

$$\Psi_f^-=\sum_k \Psi_k A_{kf}^- \tag{10}$$

where the coefficients A_{ki} and A_{kf}^- are given by

$$A_{ki}=\frac{1}{2a(E_k-E_i)}\sum_j w_{jk}(a)\left(a\frac{\mathrm{d}y_{ji}}{\mathrm{d}r}-by_{ji}\right)_{r=a} \tag{11}$$

and

$$A_{kf}^-=\frac{1}{2a(E_k-E_i-\omega)}\sum_j w_{jk}(a)\left(a\frac{\mathrm{d}y_{jf}^-}{\mathrm{d}r}-by_{jf}^-\right)_{r=a} \tag{12}$$

as discussed in BHR. The radial functions y_{ji} and y_{jf}^- describe the motion of the $(N+1)$th electron in Ψ_i and Ψ_f^- respectively, E_i is the energy of the initial state, determined as described below, and the $w_{jk}(a)$ are defined in terms of the radial basis functions

$u_{ji}(a)$ on the boundary of the internal region by

$$w_{jk}(a) = \sum_i c_{jik} u_{ji}(a). \tag{13}$$

It is important to remember that since Ψ_i and Ψ_f^- have different angular symmetries the E_k and $w_{jk}(a)$ occurring in equations (11) and (12) are not the same since they are determined by diagonalizing the Hamiltonian in equation (8) in different L–S function spaces.

To complete the development of the basic theory we must evaluate the radial functions y_{ji} and y_{jf}^- and their derivatives on the boundary of the internal region. In BHR it was shown that these functions satisfied the following coupled differential equations in the external region

$$\left(\frac{d^2}{dr^2} - \frac{l_j(l_j+1)}{r^2} + \frac{2Z}{r} + k_j^2\right) y_j(r) = 2\sum_{k=1}^{n} V_{jk}(r) y_k(r) \qquad j = 1, \ldots, n, \quad r > a \tag{14}$$

where n is the number of channel functions included in Ψ_i or in Ψ_f^-. Each element of the potential matrix $V_{jk}(r)$ can be expressed in terms of a finite inverse power series in r. This type of equation has been discussed by many authors and a general computer program for its solution has been written by Norcross (1969) and modified by Chivers (1973). We will therefore assume that a complete set of $n+n_a$ independent solutions can be calculated for all $r \geqslant a$ where n_a is the number of open channels. We define these to satisfy the asymptotic boundary conditions

$$\begin{aligned}
&v_{ij}(r) \underset{r\to\infty}{\simeq} k_i^{-1/2} \sin\theta_i \delta_{ij} + O(r^{-1}) && i = 1, \ldots, n, \quad j = 1, \ldots, n_a \\
&v_{ij}(r) \underset{r\to\infty}{\simeq} k_i^{-1/2} \cos\theta_i \delta_{ij-n_a} + O(r^{-1}) && i = 1, \ldots, n, \quad j = n_a+1, \ldots, 2n_a \\
&v_{ij}(r) \underset{r\to\infty}{\simeq} \exp(-|k_i|r)\delta_{ij-n_a} + O(r^{-1}\exp(-|k_i|r)) && i = 1, \ldots, n, \\
&\qquad\qquad j = 2n_a+1, \ldots, n+n_a
\end{aligned} \tag{15}$$

where for convenience we have listed the open channels first, and where

$$\theta_i = k_i r - \tfrac{1}{2} l_i \pi - \eta_i \ln 2k_i r + \arg\Gamma(l_i+1+i\eta_i) \qquad i = 1, \ldots, n_a. \tag{16}$$

We now expand both y_{ji} and y_{jf}^- in terms of these asymptotic basis functions. In each case they satisfy the equation

$$y_i(a) = \sum_{j=1}^{n} R_{ij}\left(a\frac{dy_j}{dr} - by_j\right)_{r=a} \qquad i = 1, \ldots, n \tag{17}$$

where the R matrices corresponding to the initial and the final states are given by

$$R_{ij} = \frac{1}{2a}\sum_k \frac{w_{ik}(a)w_{jk}(a)}{E_k - E} + R_{ij}^{\text{corr}}. \tag{18}$$

The amplitudes $w_{jk}(a)$ have already been defined by equation (13) and the correction term for the high-lying poles omitted in the first expansion can be determined using the method of Buttle (1967).

In the initial state, all channels are closed and consequently $n_a = 0$. We then have

$$y_{ji} = \sum_{k=1}^{n} v_{jk} x_k \qquad j = 1, \ldots, n, \quad a \leqslant r \leqslant \infty. \tag{19}$$

Substituting into equation (17) gives n homogeneous equations in the n coefficients x_k.

A non-trivial solution exists only if the determinant of the coefficients vanishes. This occurs at the discrete eigenvalues corresponding to the bound states of the atom. To solve these equations we write them in the form

$$\sum_{j=1}^{n} B_{ij}x_j = 0 \qquad i = 1, \ldots, n. \tag{20}$$

An unnormalized solution can be found by setting $x_1 = 1$ and solving the last $(n-1)$ equations

$$\sum_{j=2}^{n} B_{ij}x_j = -B_{i1} \qquad i = 2, \ldots, n. \tag{21}$$

The bound-state eigenenergy E_i is then given by the appropriate zero of the function

$$f(E) = \sum_{j=1}^{n} B_{1j}x_j. \tag{22}$$

This can be found using Newton's iteration method, and the corresponding solution Ψ_i normalized to give the y_{ji}. In this procedure the differential equations (14) must be solved at each stage of the iteration to yield the n basis functions v_{jk}. In practice, this method of finding the bound-state eigenvalues has proven very stable.

In the final state at least one channel is open and so we can write

$$y_{jf}^{-} = \sum_{k=1}^{n+n_a} v_{jk}x_k \qquad j = 1, \ldots, n \quad a \leqslant r \leqslant \infty. \tag{23}$$

Substituting into equation (17) yields n equations for the $n+n_a$ coefficients x_k. The remaining n_a equations required to completely determine the y_{jf}^{-} are given by the ingoing wave boundary conditions, consistent with the normalization in equations (1) and (2), which we write in matrix notation as

$$\mathbf{y}^{-} \underset{r\to\infty}{\sim} (\pi \boldsymbol{k})^{-1/2}(\sin\boldsymbol{\theta} + \cos\boldsymbol{\theta}\mathbf{K})(1 + \mathrm{i}\mathbf{K})^{-1}, \qquad n_a \text{ open channels.} \tag{24}$$

The determination of the $n_a \times n_a$ dimensional K matrix has been described in BHR. At each energy n_a independent solutions $y_{jf}^{-}, f = 1, \ldots, n_a$ can be obtained by solving simultaneously equations (17) and (24). Finally this procedure must be repeated for each total orbital angular momentum L that occurs in the final state.

To complete the evaluation of the cross section we introduce the reduced matrix elements

$$\langle \Psi_f^{-} \| M_1 \| \Psi_i \rangle = \frac{(2L+1)^{1/2}}{C_{L_i 1}(LM_L; M_{L_i}\mu)} \langle \Psi_f^{-} | M_1^{\mu} | \Psi_i \rangle \tag{25}$$

where we have used the notation of Fano and Racah (1959). When $\mu = 0$ M_1^{μ} on the right-hand side of this equation is either the dipole length operator appearing in equation (1) or the dipole velocity operator appearing in equation (2). In the calculation of this reduced matrix element we will assume that the only significant contribution comes from the internal region. This is true for the examples considered in this paper where the initial states Ψ_i are strongly bound and are thus negligibly small for $r > a$. However, for photoionization from excited states and photodetachment of negative ions a significant contribution to the matrix element will come from the external region. This contribution can be determined in terms of the solutions of the asymptotic equations (14).

The differential cross section for photoionization by light whose spherical polarization component is μ, leaving the ion in a definite $L_f S_f$ state, can be obtained by substituting equations (3) and (25) into either equations (1) or (2) suitably modified for any μ. After averaging over the initial magnetic quantum numbers and summing over the final magnetic quantum numbers we find, after some algebraic reduction, that

$$\begin{aligned}\frac{d\sigma}{d\hat{\boldsymbol{k}}} = \frac{8\pi^2\alpha a_0^2 C}{(2L_i+1)} \sum_{l_f l_{f'} L L' l} & i^{l_f - l_{f'}}(-1)^{L_f+L_i+\mu} \exp(-i\sigma_{l_f} + i\sigma_{l_{f'}}) \\ & \times \left\{\frac{(2l_f+1)(2l_{f'}+1)(2L+1)(2L'+1)}{4\pi(2l+1)}\right\}^{1/2} \\ & \times C_{l_f l_{f'}}(l0\,;00) C_{1\,1}(l0\,;-\mu\mu) W(L l_f L' l_{f'}\,; L_f l) W(1L1L'\,; L_i l) \\ & \times \langle \Psi_i \| M_1 \| \Psi_{f'}^- \rangle \langle \Psi_f^- \| M_1 \| \Psi_i \rangle Y_l^0(\hat{\boldsymbol{k}}) \end{aligned} \tag{26}$$

where $C = \omega$ in the length approximation and $C = \omega^{-1}$ in the velocity approximation. The total cross section for photoionization by unpolarized light can be obtained by integrating this equation over all ejected electron angles $\hat{\boldsymbol{k}}$ and averaging over photon polarization directions μ. In this case only the $l = 0$ term contributes and we find that

$$\sigma = \frac{8\pi^2\alpha a_0^2 C}{3(2L_i+1)} \sum_{l_f L} |\langle \Psi_f^- \| M_1 \| \Psi_i \rangle|^2. \tag{27}$$

We now expand the reduced matrix elements in equation (25) in terms of the basis functions Φ_k in equation (7). We define a reduced matrix $\mathbf{M}$ with elements

$$M_{kk'} = \langle \Phi_k \| M_1 \| \Phi_{k'} \rangle \tag{28}$$

and diagonal matrices $\mathbf{G}_i$ and $\mathbf{G}_f$ with diagonal elements

$$G_{ki} = \frac{1}{E_k - E_i}, \qquad G_{kf} = \frac{1}{E_k - E_i - \omega}. \tag{29}$$

Then the expression for the cross section becomes

$$\sigma = \frac{2\pi^2\alpha a_0^2 C}{3a^2(2L_i+1)} \sum_{l_f L} \mathbf{y}_f^{-\mathrm{T}} \mathbf{R}_f^{-1} \mathbf{w}_f \mathbf{G}_f \mathbf{V}_f^{\mathrm{T}} \mathbf{M} \mathbf{V}_i \mathbf{G}_i \mathbf{w}_i^{\mathrm{T}} \mathbf{R}_i^{-1} \mathbf{y}_i \tag{30}$$

where the V matrices are defined by equation (7), the $\mathbf{w}$ matrices by equation (13), the $\mathbf{R}$ matrices by equation (18) and the $\mathbf{y}$ matrices by equations (19) and (23). This expression is used to determine the photoionization cross sections given in § 4.

3. Description of the approximations used for neon and argon

3.1. The ionic wavefunctions

In applying the theory developed in the previous section to any atomic system it is first necessary to decide on the number and representation of the ionic states which are retained in expansion (4). In our application to neon and argon we consider the processes

$$h\nu + \mathrm{Ne}(1s^2 2s^2 2p^6\ {}^1\mathrm{S}) \begin{cases} \nearrow \mathrm{Ne}^+(1s^2 2s^2 2p^5\ {}^2\mathrm{P}) + e^-(ks, kd) \\ \searrow \mathrm{Ne}^+(1s^2 2s 2p^6\ {}^2\mathrm{S}) + e^-(kp) \end{cases} \tag{31}$$

and

$$h\nu + \mathrm{Ar}(1s^2 2s^2 2p^6 3s^2 3p^6\ {}^1S) \begin{cases} \nearrow \mathrm{Ar}^+(1s^2 2s^2 2p^6 3s^2 3p^5\ {}^2P) + e^-(ks, kd) \\ \searrow \mathrm{Ar}^+(1s^2 2s^2 2p^6 3s 3p^6\ {}^2S) + e^-(kp) \end{cases} \tag{32}$$

where the final state is $^1P^o$. In both the expansion of the initial $^1S^e$ state of the target atom and the final $^1P^o$ state given by equation (4) we retain the ^2P and ^2S ionic states. These are coupled with the wavefunction of the $(N+1)$th electron to give two coupled channels in the initial state and three coupled channels in the final state.

We carry out two types of calculation. In the first, called hereafter SC, both ionic states are represented by single configurations using the Hartree–Fock orbitals of Clementi (1965) for the ^2P ground state of the ion. In the second, called hereafter CI, we introduce additional $\overline{3s}$, $\overline{3p}$ and $\overline{3d}$ pseudo-orbitals in the case of neon and $\overline{4s}$, $\overline{4p}$ and $\overline{3d}$ pseudo-orbitals in the case of argon and we represent each ionic state as linear combinations of configurations formed from the Hartree–Fock orbitals and these pseudo-orbitals.

The pseudo-orbitals, which are defined in tables 1 and 2, are calculated, using the program of Hibbert (1975), by varying the linear coefficients and exponents to ensure orthogonality with the Hartree–Fock orbitals and to optimize the energy differences and oscillator strengths of the ionic states. In this calculation, the final results are obtained including all possible configurations, defined by tables 3 and 4. Thus, for example, the four configurations obtained by allowing one-electron excitations from the 2s and 2p shells to the $\overline{3p}$ shell in the ^2P state of neon are

$$1s^2 2s^2 2p^4\ {}^3P\ \overline{3p}, \qquad 1s^2 2s^2 2p^4\ {}^1D\ \overline{3p}, \qquad 1s^2 2s^2 2p^4\ {}^1S\ \overline{3p}, \qquad 1s^2 2p^6 \overline{3p}. \tag{33}$$

The remaining configurations in tables 3 and 4 can be easily written down remembering that the 1s shell in neon and the 1s, 2s and 2p shells in argon are always fully occupied. As expected two-electron excitations into the $\overline{3d}$ shell were found to be important particularly in the case of argon.

Table 1. Bound orbitals used in the neon calculation.

Orbital	Orbital description
1s, 2s, 2p	Clementi orbitals for $Ne^+(^2P)$
$\overline{3s}$	$(5{\cdot}62205r - 30{\cdot}1055r^2 + 23{\cdot}91867r^3)\,e^{-2{\cdot}3049r}$
$\overline{3p}$	$(12{\cdot}44329r^2 - 11{\cdot}84112r^3)\,e^{-2{\cdot}03615r}$
$\overline{3d}$	$1{\cdot}9130r^3\,e^{-2{\cdot}33277r} + 30{\cdot}03283r^3\,e^{-3{\cdot}61363r}$

Table 2. Bound orbitals used in the argon calculation.

Orbital	Orbital description
1s, 2s, 2p, 3s, 3p	Clementi orbitals for Ar^+ (^2P)
$\overline{4s}$	$(1{\cdot}4854r - 14{\cdot}5657r^2 + 27{\cdot}2106r^3 - 11{\cdot}2039r^4)\,e^{-2{\cdot}0035r}$
$\overline{4p}$	$(11{\cdot}9886r^2 - 29{\cdot}2348r^3 + 12{\cdot}6968r^4)\,e^{-2{\cdot}07058r}$
$\overline{3d}$	$4{\cdot}14319r^3\,e^{-1{\cdot}9763r} + 7{\cdot}4522r^3\,e^{-4{\cdot}01064r}$

Table 3. Configurations included in the ^2P and ^2S states of Ne^+.

	Number of configurations	
Excitation from the 2s and 2p shells	Ne^+ (^2P)	Ne^+ (^2S)
Zero-electron excitation	1	1
One-electron excitation to $\overline{3s}$ shell	2	2
One-electron excitation to $\overline{3p}$ shell	4	2
One-electron excitation to $\overline{3d}$ shell	2	1
Two-electron excitation to $\overline{3d}$ shell	10	4
Totals	19	10

Table 4. Configurations included in the ^2P and ^2S states of Ar^+.

	Number of configurations	
Excitation from the 3s and 3p shells	Ar^+ (^2P)	Ar^+ (^2S)
Zero-electron excitation	1	1
One-electron excitation to $\overline{4s}$ shell	2	2
One-electron excitation to $\overline{4p}$ shell	4	2
One-electron excitation to $\overline{3d}$ shell	2	1
Two-electron excitation to $\overline{3d}$ shell	10	4
Totals	19	10

Our results for the energies and oscillator strengths using these wavefunctions are given in tables 5 and 6. The energies for the ground states of Ne and Ar, obtained using equation (22), are also given in these tables. The CI energy differences are seen to be in good accord with the experimental results quoted by Moore (1949). Further, we see that configuration-interaction effects are most important for the oscillator strengths. Our final CI length and velocity results for Ar^+ are however still somewhat larger than the experimental value quoted by Wiese *et al* (1969). It is not clear at this time whether the theoretical CI results or the experimental result is to be preferred. In general, however, we believe that our CI ionic wavefunctions are sufficiently accurate to be used with confidence in the photoionization calculations described in the next section.

3.2. The continuum wavefunction

We have already seen that the initial bound state and final continuum state are expanded in terms of the basis functions defined by equation (4) where the $\overline{\Phi}_i$ are constructed

Table 5. Energies (au) and oscillator strengths for Ne^+ and Ne.

	SC	CI	Experiment
$E(Ne\ ^1S)$	−128·5895	−128·7136	
$E(Ne^+\ ^2P)$	−127·8176	−127·9009	
$E(Ne^+\ ^2S)$	−126·7332	−126·9039	
$\Delta E(Ne–Ne^+\ ^2P)$	0·7718	0·8005	0·7926[a]
$\Delta E(^2S–^2P)$	1·0844	0·9969	0·9889[a]
$f_L(^2S–^2P)$	0·175	0·104	0·09
$f_V(^2S–^2P)$	0·116	0·112	

[a] Moore (1949).

Table 6. Energies (au) and oscillator strengths for Ar^+ and Ar.

	SC	CI	Experiment
$E(Ar\ ^1S)$	−526·8313	−526·9676	
$E(Ar^+\ ^2P)$	−526·2761	−526·3855	
$E(Ar^+\ ^2S)$	−525·5970	−525·8873	
$\Delta E(Ar–Ar^+\ ^2P)$	0·5552	0·5821	0·5792[a]
$\Delta E(^2S–^2P)$	0·6773	0·4982	0·4954[a]
$f_L(^2S–^2P)$	0·3118	0·0297	0·0089[b]
$f_V(^2S–^2P)$	0·1936	0·0254	

[a] Moore (1949).
[b] Wiese *et al* (1969).

from the ^2S and ^2P ionic states. We now obtain s-, p- and d-wave continuum orbitals u_{ij} by solving equations (5) and (6) both for neon and argon. The zero-order potential which we choose is

$$V(r) = \frac{2}{r} + \frac{2(Z-1)}{r} e^{-\alpha r} \tag{34}$$

which has the correct form both near the nucleus and asymptotically and we take α so that equation (5) gives bound state eigenenergies which are in reasonable agreement with experiment. We orthogonalize these continuum orbitals to the Hartree–Fock orbitals in equation (5) and in the CI calculation we then orthogonalize to the additional pseudo-orbitals, using the method of Schmidt described in detail by Berrington *et al* (1974). We find excellent convergence both for the SC and the CI calculations with less than 15 continuum orbitals included in each channel.

The number of bound configurations ϕ_i retained in the second expansion in equation (4) depends on whether we are using the SC or the CI approach. In the SC approach we include the minimum number of configurations to ensure that our orthogonalization procedure does not lead to the omission of basic capture terms. This involves including just the $1s^22s^22p^6\ ^1S$ configuration in the neon ^1S ground state calculation and the $1s^22s^22p^63s^23p^6\ ^1S$ configuration in the argon ^1S ground state calculation. In the CI approach we include all bound configurations consistent with the excitations included in the ionic states. These configurations are defined by tables 7 and 8. We see that all

Table 7. Bound configurations included in initial and final states of neon.

Excitation from the 2s and 2p shells	Number of configurations	
	Ne (^{1}S) initial state	Ne (^{1}P^o) final state
Zero-electron excitation	1	0
One-electron excitation to $\overline{3s}$	1	1
One-electron excitation to $\overline{3p}$	1	1
One-electron excitation to $\overline{3d}$	0	1
Two-electron excitation to $\overline{3s}$	2	1
Two-electron excitation to $\overline{3p}$	4	3
Two-electron excitation to $\overline{3d}$	4	3
One-electron excitation to $\overline{3s}$ + one-electron excitation to $\overline{3p}$	2	4
One-electron excitation to $\overline{3s}$ + one-electron excitation to $\overline{3d}$	1	2
One-electron excitation to $\overline{3p}$ + one-electron excitation to $\overline{3d}$	2	7
Two-electron excitation to $\overline{3d}$ + one-electron excitation to $\overline{3s}$	4	10
Two-electron excitation to $\overline{3d}$ + one-electron excitation to $\overline{3p}$	10	23
Three-electron excitation to $\overline{3d}$	4	11
Total	36	67

possible one- and two-electron excitations are included and in addition three-electron excitations involving the $\overline{3d}$ shell are also included. Again, the 1s shell in neon and the 1s, 2s and 2p shells in argon are fully occupied in all configurations. Clearly the inclusion of these terms allows for configuration-interaction effects when all the electrons are in the internal region which are omitted in the usual close-coupling approximation.

3.3. Brief comments on the computation

The calculations were carried out on the ICL 1906A at the Atlas Computer Laboratory. First, all possible radial integrals involving the atomic and continuum orbitals were calculated and stored on magnetic tape. This part of the calculation took about 25–30% of the total computer time. Next the Hamiltonian matrix elements $(\Phi_k|H|\Phi_{k'})$ in equation (8) were calculated both for the initial ^{1}S^e and the final ^{1}P^o states. Because of the time taken by the angular integrals this part of the calculation took another 25–30% of

Table 8. Bound configurations included in initial and final states of argon.

Excitation from the 3s and 3p shells	Number of configurations	
	Ar (^{1}S)	Ar (^{1}P^o)
Zero-electron excitation	1	0
One-electron excitation to $\overline{4s}$	1	1
One-electron excitation to $\overline{4p}$	1	1
One-electron excitation to $\overline{3d}$	0	1
Two-electron excitation to $\overline{4s}$	2	1
Two-electron excitation to $\overline{4p}$	4	3
Two-electron excitation to $\overline{3d}$	4	3
One-electron excitation to $\overline{4s}$ + one-electron excitation to $\overline{4p}$	2	4
One-electron excitation to $\overline{4s}$ + one-electron excitation to $\overline{3d}$	1	2
One-electron excitation to $\overline{4p}$ + one-electron excitation to $\overline{3d}$	2	7
Two-electron excitation to $\overline{3d}$ + one-electron excitation to $\overline{4s}$	4	10
Two-electron excitation to $\overline{3d}$ + one-electron excitation to $\overline{4p}$	10	23
Three-electron excitation to $\overline{3d}$	4	11
Total	36	67

the total computer time. Finally, the Hamiltonian matrices were diagonalized and the cross sections calculated at more than one hundred energy points in each case. The time in this part of the calculation was almost entirely spent solving the asymptotic equations (14) which had to be carried out at each energy point considered.

4. Results

4.1. Autoionizing states

It is well known that Rydberg series of autoionization states or resonances converge onto all excited states of the N-electron ion. In the case of neon and argon we are interested in the following series

$$\mathrm{Ne}(1s^2 2s 2p^6 np\ ^1P^o) \qquad n = 3, 4, \ldots \tag{35}$$

and

$$\mathrm{Ar}(1s^2 2s^2 2p^6 3s 3p^6 np\ ^1P^o) \qquad n = 4, 5, \ldots \tag{36}$$

which are formed as intermediate states in photoionization from the ground state in equations (31) and (32) respectively and converge onto the ^2S threshold.

We have carried out calculations near the lowest two autoionizing states both for neon and argon. We show our results near the $n = 3$ state in neon in figure 1 where we compare the length and velocity results both for the SC and the CI approximations.

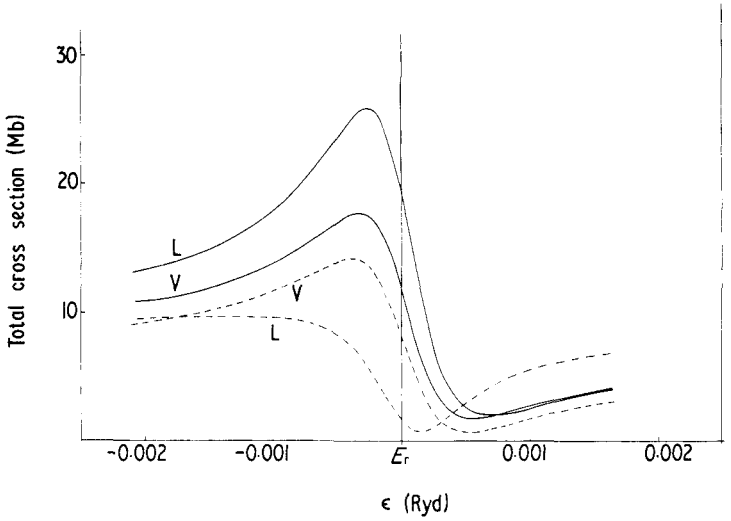

Figure 1. The photoionization cross section near the neon $1s^22s2p^63p\ ^1P^o$ resonance. The broken curves are the length (L) and velocity (V) SC results and the full lines are the length and velocity CI results.

The SC results are in accord with the earlier work of Luke (1973) who used a similar approximation. However, we see that the length and velocity values are not in good agreement with each other. Including CI brings the length and velocity results into much better accord and, as we shall see below, significantly improves the agreement with experiment. The reasonable agreement between the CI length and velocity results is maintained along the Rydberg series, and we illustrate this in the case of the $n = 4$ state in figure 2.

Similar results for the first two autoionizing states in argon are shown in figure 3 and 4. Here the SC results are completely wrong both with regard to shape and width. However the inclusion of CI brings the length and velocity results into very good agreement with each other and also with experiment.

In order to compare these results with experiment we analyse them using the parametrization introduced by Fano (1961) and Fano and Cooper (1965). In the neighbourhood of an isolated autoionizing state the photoionization cross section can be written in the form

$$\sigma = \sigma_a \frac{(\epsilon + q)^2}{1 + \epsilon^2} + \sigma_b \tag{37}$$

where q is called the line profile index, which defines the shape of the absorption cross section,

$$\epsilon = \frac{E - E_r}{\frac{1}{2}\Gamma} \tag{38}$$

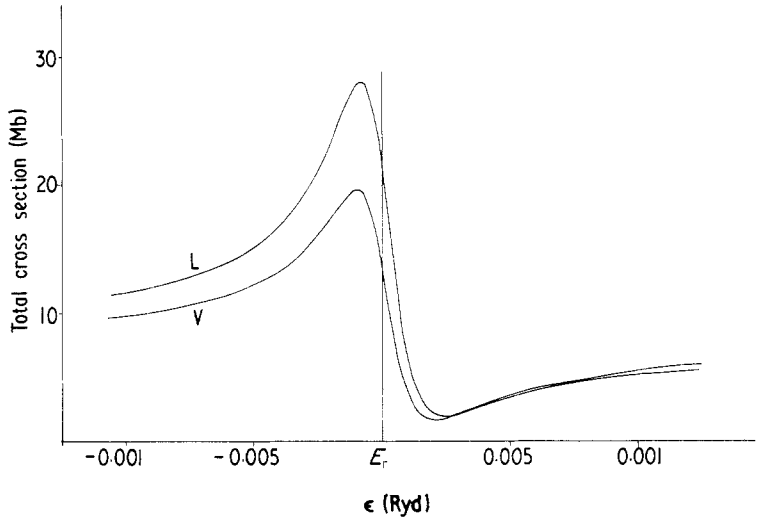

Figure 2. The photoionization cross section near the neon $1s^2 2s 2p^6 4p\ {}^1P^o$ resonance. The CI length (L) and velocity (V) results are shown.

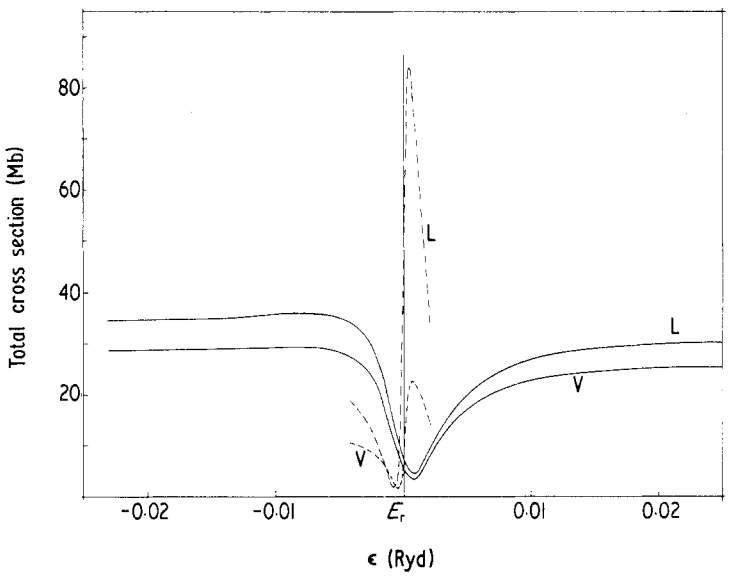

Figure 3. The photoionization cross section near the argon $1s^2 2s^2 2p^6 3s 3p^6 4p\ {}^1P^o$ resonance. The same four approximations are used as in figure 1.

and σ_a and σ_b are slowly varying background cross sections. It is also convenient to define a correlation coefficient

$$\rho^2 = \frac{\sigma_a}{\sigma_a + \sigma_b} \tag{39}$$

which gives the proportion of the continuum which interacts with the autoionizing state. We now obtain the width Γ and the position E_r by fitting the sum of the scattering

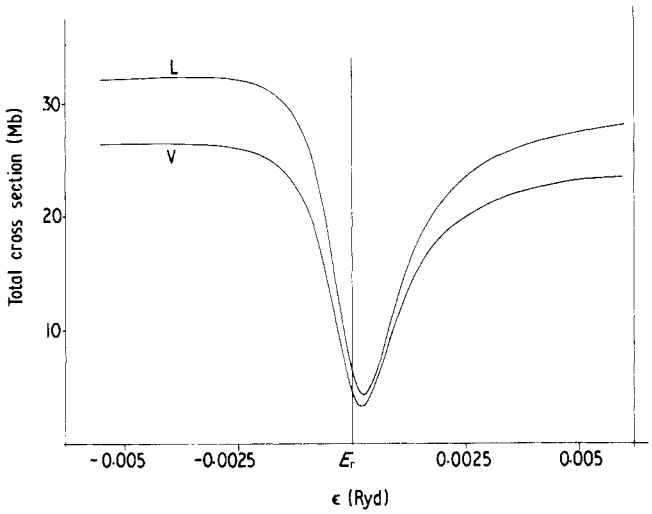

Figure 4. The total photoionization cross section near the argon $1s^22s^22p^63s3p^65p\ ^1P^o$ resonance. The CI length and velocity results are shown.

eigenphase shifts in the final state as in the work of Burke and McVicar (1965). We then obtain the parameters σ_a, σ_b and q by fitting equation (37) to the calculated cross sections shown in figures 1–4.

We compare our results for these parameters with experiment in tables 9 and 10. In the case of neon the experimental results are those of Codling *et al* (1967) and in the case of argon the results are those of Madden *et al* (1969). These both used the synchrotron radiation source at the NBS in Washington, DC. We see that in all cases the CI calculation gives a very significant improvement over the SC calculation. This is particularly marked in the case of q both for neon and argon and for Γ in the case of argon. Our final results are in satisfactory agreement with experiment in all cases. In conclusion, it is clear from this work that the study of resonance parameters provides a very sensitive test of the theory.

4.2. Total photoionization cross section

We present our SC and CI results calculated in the dipole length and velocity approximations for neon in figure 5. The energy region just below the ^2S threshold containing the resonances discussed in the previous subsection is omitted for clarity. Our SC length result is again in good agreement with Luke (1973). We see that including CI brings the length and velocity results into satisfactory agreement over the full energy range considered. We then compare our CI length calculation with the experimental results of Samson (1965), the random-phase approximation with exchange (RPAE) of Amusia *et al* (1971) and the SC length results of Luke (1973) (figure 6). Our calculations agree best with experiment at low energies. At higher energies our results are almost identical to the RPAE approximation and both show a small step in the neighbourhood of the ^2S threshold arising from the new channel.

Similar calculations have been carried out for argon and are presented in figures 7 and 8. In figure 7 we see that the length and velocity CI results are in reasonable agreement. In figure 8 we compare our length CI results with the experimental measurements

Table 9. Neon resonance parameters.

	$1s^2 2s 2p^6 3p\ ^1P^o$			$1s^2 2s 2p^6 4p\ ^1P^o$	
	SC	CI	Experiment	CI	Experiment
Quantum defect	0·814	0·824	0·845	0·808	0·829
Γ (eV)	0·0121	0·0117	0·013(±0·002)	0·0038	0·0045(±0·0015)
q length	−0·34	−1·61	−1·6(±0·2)	−1·75	−1·6(±0·3)
q velocity	−1·16	−1·30		−1·46	
ρ^2 length	0·93	0·76	0·70(±0·07)	0·76	0·70(±0·07)
ρ^2 velocity	0·91	0·77		0·77	

Table 10. Argon resonance parameters.

	$1s^2 2s^2 2p^6 3s 3p^6 4p\ ^1P^o$			$1s^2 2s^2 2p^6 3s 3p^6 5p\ ^1P^o$	
	SC	CI	Experiment	CI	Experiment
Quantum defect	1·639	1·678	1·723	1·651	1·690
Γ (eV)	0·015	0·068	0·080(±0·005)	0·0243	0·0282(±0·0013)
q length	1·58	−0·33	−0·22(±0·05)	−0·26	−0·21(±0·02)
q velocity	0·90	−0·29		−0·22	
ρ^2 length	0·905	0·855	0·86(±0·04)	0·85	0·83(±0·02)
ρ^2 velocity	0·899	0·861		0·86	

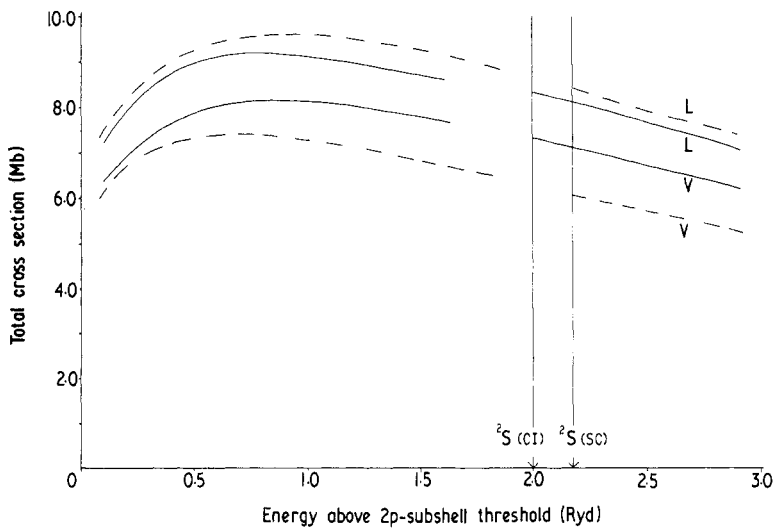

Figure 5. The neon total photoionization cross section calculated in four approximations. The same notation is used as in figure 1.

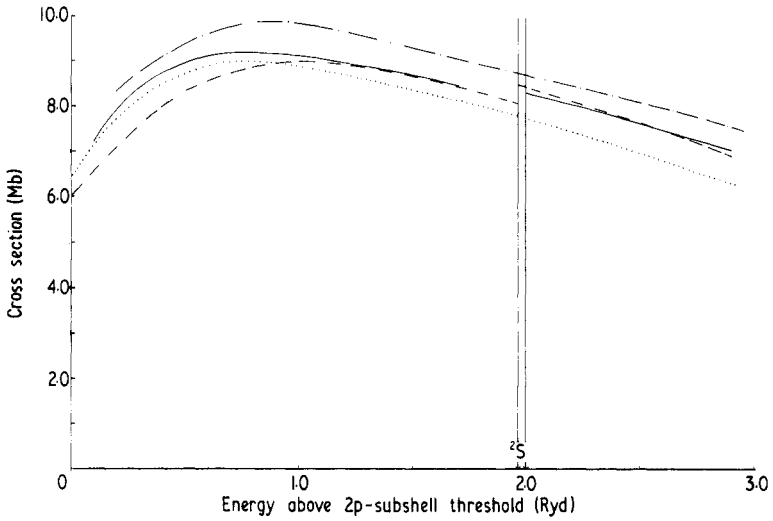

Figure 6. Comparison of theory and experiment for the total photoionization cross section in neon. The full curve is the length CI calculation of this paper. The dotted curve is the experimental results of Samson (1965), the broken curve is the RPAE calculations of Amusia *et al* (1971) and the dash–dot curve is the calculation of Luke (1973).

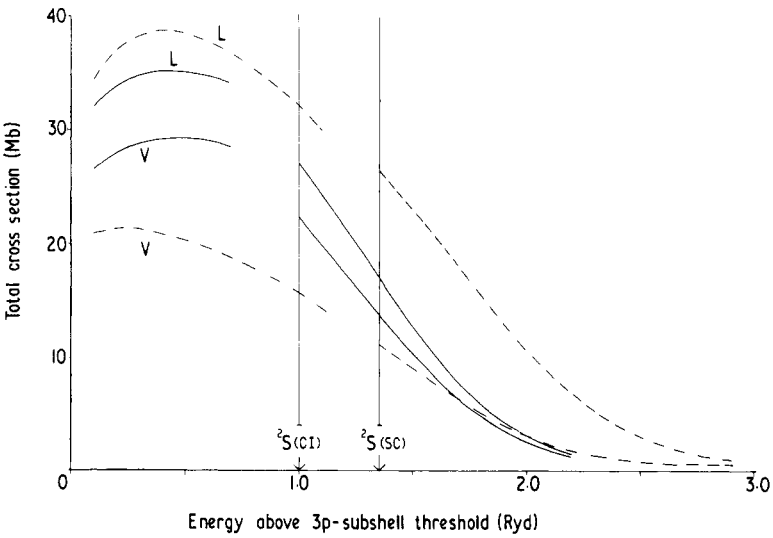

Figure 7. The argon total photoionization cross sections calculated in four approximations. The same notation is used as in figure 1.

of Samson (1965), the K-matrix results of Starace (1970) and the RPAE results of Amusia *et al* (1971). The calculation of Starace included intrachannel coupling in the final kd channel in equation (32) but did not include any interchannel coupling with the ks and kp channels. On the other hand interchannel mixing was effectively included in the random-phase approximations of Amusia *et al* and Lin (1974) as well as of course in our calculation. Again our results are in better agreement with experiment at low energies but are somewhat higher than experiment at higher energies although the overall picture is considered satisfactory.

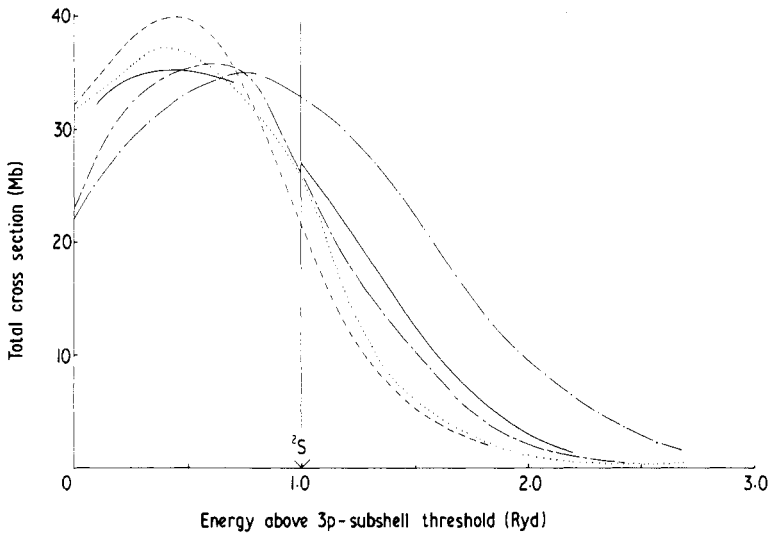

Figure 8. Comparison of theory and experiment for the total photoionization cross section in argon. The full curve is the length CI calculation of this paper. The dotted curve is the experimental results of Samson (1965), the broken curve is the RPAE calculations of Amusia *et al* (1971), the dash–dot curve is the *K*-matrix calculations of Starace (1970) and the short and long dashed curve is the SRPAE calculations of Lin (1974).

In summary, we find agreement to better than 15% between our CI length and velocity results. Further our length results, which agree best with experiment, give a satisfactory picture of the total photoionization cross section over an extended energy range.

4.3. Photoionization of the s subshell

We conclude by presenting our results for the photoionization of the 2s subshell in neon and the 3s subshell in argon. These results provide a more sensitive test of the theory since they depend more on the approximation than the total cross section results presented in the previous subsection.

We compare our length CI results for neon in figure 9 with the experimental results of Samson and Gardner (1974), Wuilleumier and Krause (1974) and West and Houlgate (1975)† and with the Hartree–Fock calculations of Kennedy and Mansen (1972) and the RPAE calculations of Amusia *et al* (1972). Above 3·5 Ryd our results are obtained by averaging the calculated cross sections over many resonances as shown in figure 10. These resonances arise from terms included in the second expansion in equation (4) which allow for electron-correlation effects when the ejected electron is still within the charge distribution of the ion. They simulate to some extent the open channels neglected in the first expansion. In the theory of nuclear reactions, averages of this sort are used to define a complex optical potential as described by Brown (1959). Clearly there is some ambiguity in the averaging procedure but it is unlikely to produce an error of more than 10%. Returning to the comparison with experiment and other calculations in figure 9, we see that our results are close to those of Amusia *et al* at low energies and are considerably lower than the Hartree–Fock results. However they do agree well over the whole energy range with the recent results of West and Houlgate (1975)† which

† Private communication from Dr J B West.

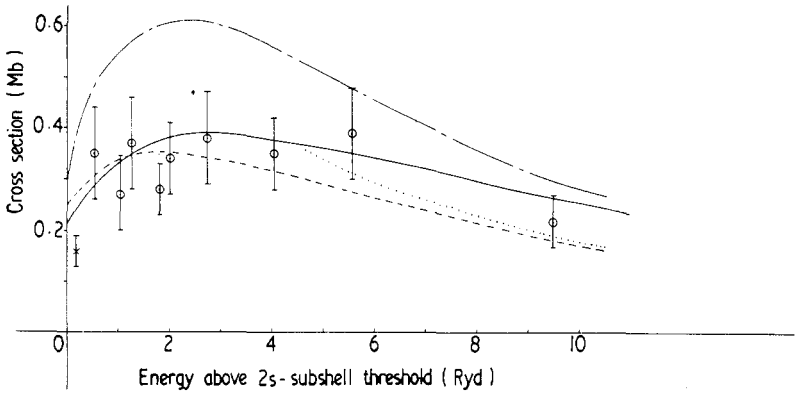

Figure 9. The neon 2s-subshell photoionization cross section. The full curve is the length CI calculations of this paper. The cross is the experimental result of Samson and Gardner (1974), the dotted curve is the experimental results of Wuilleumier and Krause (1974), the circles are the experimental results of West and Houlgate (1975)†, the short and long dashed curve is the HF calculations of Kennedy and Mansen (1972) and the broken curve is the RPAE calculations of Amusia *et al* (1972).

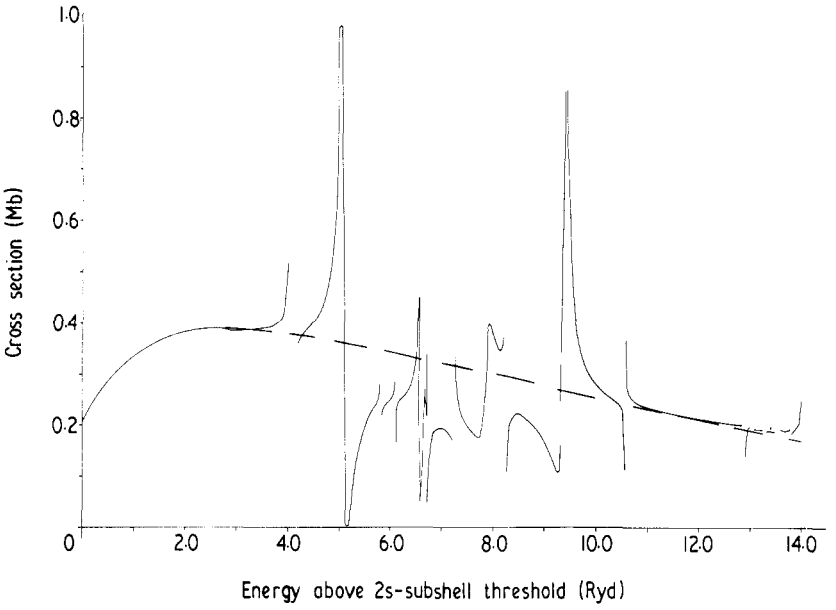

Figure 10. The neon 2s-subshell photoionization cross section calculated in the CI length approximation. The full curve is the calculated values and the broken line is the average.

extrapolate smoothly to the higher energy results of Wuilleumier and Krause. We remark here that our velocity CI results, which are not shown, lie consistently some 15–20% lower than the length results over the energy range considered.

† Private communication from Dr J B West.

Finally, we compare our length CI results for argon in figure 11 with the experimental data of Samson and Gardner (1974), Houlgate *et al* (1974) and Marr *et al* (1975)† and with the Hartree–Fock calculations of Cooper and Mansen (1969), the RPAE calculations of Amusia *et al* (1972) and the SRPAE calculations of Lin (1974). The important feature of this cross section is the minimum which occur at about 1 Ryd above threshold. Since it arises from the coupling between the kp and the kd continua in equation (32) it does not appear in the Hartree–Fock approximation but is correctly given in all four of our approximations. At the higher energies our results are again obtained by averaging over resonance structure as in the case of neon. Our results are a little too high at the lowest energy but agree, within the errors, with experiment at the higher energies shown.

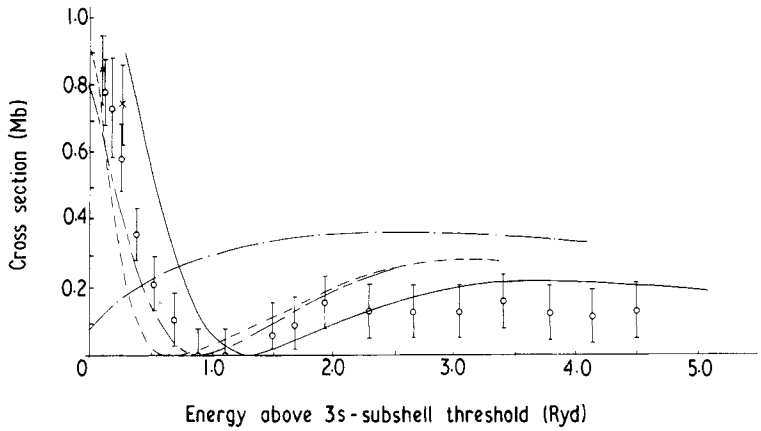

Figure 11. The argon 3s-subshell photoionization cross section. The full curve is the length CI calculations of this paper. The crosses are the experimental results of Samson and Gardner (1974), the circles are the experimental data of Marr *et al* (1975)†, the dash–dot curve is the HF calculations of Cooper and Mansen (1969), the broken curve is the RPAE calculations of Amusia *et al* (1972) and the short and long dashed curve is the SRPAE approximation of Lin (1974).

5. Conclusions

The calculations for neon and argon presented in this paper show that the R-matrix method can give quantitative agreement with experiment. The method can be systematically improved by including further configuration-interaction effects in the wavefunction and the only limitation in the accuracy in the low-energy region comes from the computer time required. At higher energies, we have shown that reasonable results can be obtained by averaging over resonances representing the channels omitted from the expansion. However this averaging procedure, suggested by optical-model theory, requires further study before it can be used with confidence in all situations. We conclude by reiterating the point made in the introduction that these calculations on a previously well studied system give us confidence in using the R-matrix method and the associated computer programs on other systems. The results of such a study are given in the following paper on the photoionization of aluminium.

† Private communication from Dr G V Marr.

Acknowledgments

One of us, KT, wishes to thank the Northern Ireland Department of Education for the award of a postgraduate studentship. The computer time used was granted by the Science Research Council at the Atlas Computer Laboratory. Finally, the research was supported by the US Office of Naval Research under Contract N00014-69-C-0035.

We are grateful to Dr G V Marr and J B West for sending us the latest data on neon and argon obtained by Drs Houlgate and West using the synchroton radiation source at the Daresbury Laboratory.

References

Allison D C S, Burke P G and Robb W D 1972 *J. Phys.* B: *Atom. Molec. Phys.* **5** 55–65
Amusia M Ya, Cherepkov N A and Chernysheva L V 1971 *Zh. Eksp. Teor. Fiz.* **60** 160 (*Sov. Phys.–JETP* **33** 90–6)
Amusia M Ya, Ivanov V K, Cherepkov N A and Chernysheva L V 1972 *Phys. Lett.* **40A** 361–2
Berrington K A, Burke P G, Chang J J, Chivers A T, Robb W D and Taylor K T 1974 *Comp. Phys. Commun.* **8** 149–98
Brown G E 1959 *Rev. Mod. Phys.* **31** 893–919
Burke P G, Hibbert A and Robb W D 1971 *J. Phys.* B: *Atom. Molec. Phys.* **4** 153–61
Burke P G and McVicar D D 1965 *Proc. Phys. Soc.* **86** 989–1006
Burke P G and Robb W D 1975 *Advances in Atomic and Molecular Physics* vol 11, ed D R Bates and B Bederson (New York and London: Academic Press) pp 143–214
Buttle P J A 1967 *Phys. Rev.* **160** 719–29
Chivers A T 1973 *Comp. Phys. Commun.* **5** 416
Clementi E 1965 *IBM J. Res. Dev. Suppl.* **9** 2
Codling K, Madden R P and Ederer D L 1967 *Phys. Rev.* **155** 26–37
Cooper J W and Mansen S T 1969 *Phys. Rev.* **177** 157–63
Fano U 1961 *Phys. Rev.* **124** 1866–78
Fano U and Cooper J W 1965 *Phys. Rev.* **137** A1364–79
—— 1968 *Rev. Mod. Phys.* **40** 441–507
Fano U and Racah G 1959 *Irreducible Tensorial Sets* (New York: Academic Press)
Henry R J W and Lipsky L 1967 *Phys. Rev.* **153** 51–6
Hibbert A 1975 *Comp. Phys. Commun.* **9** 141–72
Houlgate R G, West J B, Codling K and Marr G V 1974 *J. Phys.* B: *Atom. Molec. Phys.* **7** L470–3
Kennedy D J and Mansen S T 1972 *Phys. Rev.* A **5** 227–47
Lin C D *Phys. Rev.* A **9** 181–6
Luke T M 1973 *J. Phys.* B: *Atom. Molec. Phys.* **6** 30–41
Madden R P, Ederer D L and Codling K 1969 *Phys. Rev.* **177** 136–50
Moore C E 1949 *Atomic Energy Levels NBS Circular* No 467 (Washington, DC: US Govt Printing Office)
Norcross D W 1969 *Comp. Phys. Commun.* **1** 88–96
Robb W D 1970 *Comp. Phys. Commun.* **1** 457–64
Rose M E 1957 *Elementary Theory of Angular Momentum* (New York: Wiley) Appendix III
Samson J A R 1965 *J. Opt. Soc. Am.* **55** 935–7
Samson J A R and Gardner J L 1974 *Phys. Rev. Lett.* **33** 671–3
Wiese W L, Smith M W and Miles B M 1969 *Atomic Transition Probabilities II, Sodium through Calcium* NSRDS–NBS Circular No 22 (Washington, DC: US Govt Printing Office)
Wuilleumier F and Krause M O 1974 *Phys. Rev.* A **10** 242–58